mathematics

Article

Semi-Active Suspension Control Strategy Based on Negative Stiffness Characteristics

Yanlin Chen [1,†], Shaoping Shen [1,*,†], Zhijie Li [1], Zikun Hu [1] and Zhibin Li [2]

[1] Department of Automation, Xiamen University, Xiamen 361005, China; yanlinchen@stu.xmu.edu.cn (Y.C.); lizhijie@stu.xmu.edu.cn (Z.L.); zikunhu@stu.xmu.edu.cn (Z.H.)
[2] College of Electrical Engineering and Automation, Shandong University of Science and Technology, Qingdao 266590, China; zhibin.li@sdust.edu.cn
* Correspondence: shen_shaoping@xmu.edu.cn
† These authors contributed equally to this work.

Abstract: This paper investigates the potential of negative stiffness suspensions for enhanced vehicle vibration isolation. By analyzing and improving traditional control algorithms, we propose and experimentally validate novel skyhook, groundhook, and hybrid control strategies for suspensions with negative stiffness characteristics. We establish pavement models, incorporate negative stiffness into suspension modeling, and develop a performance evaluation index. Our research identifies shortcomings of classical semi-active control algorithms and introduces a new band selector to combine improved control methods. Simulation results demonstrate that the proposed semi-active suspension control strategy based on negative stiffness effectively reduces body vibration and enhances vehicle ride performance.

Keywords: negative stiffness; semi-active suspension; damping control; hybrid control

MSC: 93-05; 93-10

Citation: Chen, Y.; Shen, S.; Li, Z.; Hu, Z.; Li, Z. Semi-Active Suspension Control Strategy Based on Negative Stiffness Characteristics. *Mathematics* **2024**, *12*, 3346. https://doi.org/10.3390/math12213346

Academic Editors: Montserrat Gil-Martinez, Ramón Vilanova Arbós and Marian Barbu

Received: 19 September 2024
Revised: 22 October 2024
Accepted: 24 October 2024
Published: 25 October 2024

1. Introduction

1.1. Background

Vehicle suspension systems are paramount in determining ride comfort, handling, and overall vehicle stability [1]. They serve to isolate vibrations induced by road surface irregularities, therefore enhancing passenger comfort and protecting vehicle components from excessive wear [2,3]. As automotive technology advances, there is an increasing demand for innovative suspension solutions that can effectively address the challenges posed by diverse driving conditions [4,5]. The vibration isolation mechanism of a negative stiffness suspension system represents an innovative approach in the realm of vehicle dynamics, particularly for enhancing ride comfort and stability under varying road conditions [6,7]. This nonlinear vibration isolation device has shown significant promise in improving the effectiveness of vibration attenuation, especially in the low-frequency range, which is critical for passenger comfort during typical driving scenarios [8].

Pioneering work by Eijk et al. [9] first integrated negative stiffness into the design of vehicle suspensions, effectively reducing the overall stiffness of the system and, therefore, enhancing its vibration isolation capabilities. Building upon this foundation, the works in [10] developed a semi-active suspension system incorporating negative stiffness elements, validated through both theoretical derivation and experimental testing, which demonstrated marked improvements in ride quality. Furthermore, the study of [11] investigated the dynamic behavior of a nonlinear suspension system featuring negative stiffness, deriving the governing equations and analyzing the frequency response under harmonic excitation using advanced mathematical techniques. In a similar vein, the works by [12] explored the application of a bending-mounted spring roller mechanism as a negative

stiffness calibrator in conjunction with conventional linear springs, leading to the design of a passive nonlinear isolator. Their analysis provided insights into the dynamic characteristics and performance metrics of the isolator. The study in [13] proposed a novel vibration absorber that utilizes both positive and negative stiffness elements in parallel, leveraging the principle of counteraction to achieve an arbitrarily low effective stiffness. This innovative design significantly enhances the system's vibration isolation performance.

Negative stiffness in a vehicle suspension system refers to a characteristic where the restoring force generated by the suspension system opposes the direction of displacement. The authors of [14] further contributed to this field by examining a dual-stiffness vibration isolation system, which combines positive and negative stiffness elements to achieve a higher support stiffness while maintaining lower motion stiffness. Their findings indicated that the natural frequency of the system could be effectively manipulated by adjusting the forces acting on the negative stiffness mechanism, leading to substantial improvements in vibration isolation efficacy. Despite the growing body of research surrounding negative stiffness structures [15–25], there remains a notable gap in the literature regarding their application in the design of suspension systems for construction machinery vehicles. This highlights the urgent need for a focused investigation into the development of an accurate seat suspension system that incorporates negative stiffness characteristics. Such a system must be tailored to the specific spatial constraints of the cab seat while also optimizing its dynamic performance [26,27]. This study aims to address these challenges by exploring the design parameters and dynamic characteristics of a negative stiffness suspension system, ultimately contributing to enhanced operator comfort and vehicle performance. Negative stiffness suspensions offer a promising alternative to traditional suspension designs by utilizing mechanisms that counteract the forces exerted during vehicle motion [28]. This unique property allows for an enhanced dynamic response, potentially leading to improved ride quality and handling characteristics [29]. The primary objective of this study is to analyze and refine existing control algorithms to fully exploit the benefits of suspensions with negative stiffness characteristics [30].

To achieve this, we propose a comprehensive framework that includes the development of enhanced control strategies. Specifically, we introduce improved skyhook control, ground control, and hybrid control algorithms that are specifically tailored for suspensions exhibiting negative stiffness properties. These control algorithms aim to optimize the suspension's response to varying road conditions, therefore maximizing vibration isolation and overall vehicle performance. To rigorously evaluate the proposed methods, this paper establishes detailed models for various pavement types, which serve as the foundation for our analysis. By incorporating negative stiffness characteristics into the traditional suspension model, we create a more accurate representation of real-world driving scenarios. Additionally, we propose a performance evaluation index that quantitatively assesses the effectiveness of the suspension system, allowing for a systematic comparison of different control strategies. A critical aspect of our research involves the analysis of classical semi-active control algorithms. By identifying their limitations, we highlight the need for more advanced approaches that can better accommodate the complexities of modern driving environments. To address this gap, we introduce a novel band selector designed to synergistically combine the improved control methods, therefore enhancing the overall performance of the suspension system.

The simulation results presented in this paper provide compelling evidence that the proposed semi-active suspension control method, based on the negative stiffness mechanism, effectively reduces body vibrations and significantly improves vehicle driving performance. This research not only contributes to the understanding of advanced suspension systems but also paves the way for future innovations in automotive suspension technology. Ultimately, our findings aim to enhance safety, comfort, and driving enjoyment for users across a variety of road conditions. The main contributions of this paper are as follows:

- First, various system models necessary for the study are developed. Modeling real-world road conditions, including speed bumps and other irregularities, random

road excitation and bump models are established. Sweep frequency and sinusoidal signals are also developed for analyzing the frequency response of the suspension system. The definition and properties of stiffness are introduced and applied to a conventional stiffness suspension model, enabling the development of a negative stiffness suspension model.

- Subsequently, the improved skyhook and groundhook control algorithms for the negative stiffness suspension system are designed. This involves analyzing the control principles of traditional skyhook and groundhook control theory and modifying them in light of the dynamic characteristics of the negative stiffness semi-active suspension. Two improved skyhook and groundhook control methods are then designed. Simulink models are developed and tested for both improved control methods. Comparative analyses are performed using simulations including passive, skyhook and groundhook, and negative stiffness passive control approaches, evaluating their respective performances under various metrics to assess the advantages and disadvantages of each control strategy.
- Finally, a hybrid control algorithm for the negative stiffness suspension system is designed. A comparative analysis of several established semi-active control algorithms reveals their limitations. Due to the distinct dynamic characteristics of negative stiffness suspensions compared to conventional designs, existing control algorithms proved inadequate. Leveraging the previously developed improvs sky-ground control method, a novel frequency selector is designed to combine the two control approaches. Simulation experiments demonstrated that the proposed hybrid control method effectively enhances vehicle ride comfort. The proposed control method improves the comfort and stability of the vehicle by effectively suppressing vehicle body vibration compared with the works from [5,8] based on the proposed hybrid control methods.

1.2. Problem Formulation

The principle of skyhook control was first proposed by the study of Karnopp in the 20th century, using a dampener connected between the imaginary sky and the body to suppress the vibration of the body. The principle is to design and install an ideal skyhook damper between the body and the imaginary sky. The sky remains absolutely stationary, and the ideal skyhook damper can suppress the vertical motion of the body, thus making the body more stable and improving the comfort and smoothness of the vehicle during driving. Figure 1 shows the quarter-vehicle suspension dynamics model with skyhook control.

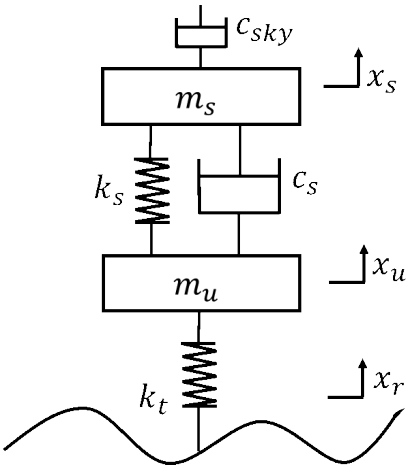

Figure 1. Control quarter suspension model.

The kinetic equations are established as follows:

$$\begin{cases} m_s\ddot{x}_s + c_s(\dot{x}_s - \dot{x}_u) + k_s(x_s - x_u) + c_{sky}\dot{x}_s = 0 \\ m_u\ddot{x}_u - c_s(\dot{x}_s - \dot{x}_u) - k_s(x_s - x_u) + k_t(x_u - x_r) = 0 \end{cases} \quad (1)$$

where c_{sky} is the damping coefficient in skyhook control, k_s is the suspension spring stiffness, m_s is the spring-loaded mass, m_u is the unsprung mass, k_t is the equivalent tire stiffness, and c_s is the inherent damping coefficient of the suspension.

After the principle of skyhook control was proposed, the theory of groundhook control was also mentioned by authors in [31], and the skyhook control and groundhook control appeared almost together in the discussion involving vehicle suspension control.

In general research, scholars mainly study the direction that can make the suspension provide better ride comfort for the vehicle, and fewer studies utilize the characteristics of the actuators in the suspension to improve road surface adhesion. In recent years, scholars through vehicle chassis integrated control research found that the improvement of road surface adhesion and even handling stability of the suspension system is also worthy of in-depth research. The principle of groundhook control is similar to that of skyhook control, which is an idealized suspension structure design scheme, and in practice, the vehicle cannot realize the damping connection with the ground; the difference is that the main idea of groundhook control theory is to connect the unsprung mass with the ground using dampers. Of course, the nature of the ground is the same as the nature of the "ideal sky" in skyhook control in order to be able to consume the energy generated by the vibration of the parts connected to it. This method effectively reduces the vibration energy of the wheels, resulting in a reduction in the vibration displacement of the wheels and an improvement in the adhesion of the wheels to the road surface.

We model its quarter-vehicle suspension dynamics as in Figure 2.

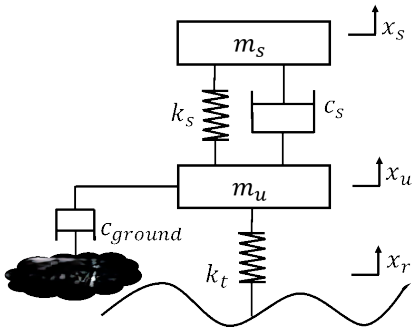

Figure 2. Ideal floor shed suspension model.

Establish the dynamics equation of this suspension as:

$$\begin{cases} m_s\ddot{x}_s + c_s(\dot{x}_s - \dot{x}_u) + k_s(x_s - x_u) = 0 \\ m_u\ddot{x}_u - c_s(\dot{x}_s - \dot{x}_u) - k_s(x_s - x_u) + k_t(x_u - x_r) + F_d = 0 \end{cases} \tag{2}$$

where F_d is the ideal damping force, $F_d = c_{ground}\dot{x}_u$.

There are also methods, such as switched groundhook control and linear groundhook control in groundhook control. The switched ground-shed damping control is a control law that implements switching based on the direction of the unsprung displacement $\dot{x}_u$ and the suspension deformation velocity $(\dot{x}_s - \dot{x}_u)$ with the following expression:

$$c_{ground} = \begin{cases} c_{\min}, \dot{x}_u(\dot{x}_s - \dot{x}_u) \le 0 \\ c_{\max}, \dot{x}_u(\dot{x}_s - \dot{x}_u) > 0 \end{cases} \tag{3}$$

where $c_{\min}$ and $c_{\max}$ are the minimum and maximum damping coefficients that can be provided by the controlled dampers, respectively. The control law is performed by a switching controller, and the controlled damper coefficient is converted to the maximum damping coefficient when the tire velocity $\dot{x}_u$ and the suspension deformation velocity $\dot{x}_s - \dot{x}_u$ are in the same direction, and the opposite is converted to the minimum damping coefficient. Under this control strategy, the damper has only two damping states, which is also easier to implement in engineering.

At this stage, the research for vehicle suspension systems is mainly divided into two aspects: one is the research of suspension structure, and the other is the research of suspension control algorithm. We further carry out the research of control strategy according to the relevant results in [4,21].

2. The Design of Skyhook and Groundhook Semi-Active Controller Based on Negative Stiffness

According to the mechanical properties of the damper, we know that the damping force is always in the opposite direction of its relative motion speed and proportional to its magnitude. The main function of the damper in the suspension is to absorb energy to minimize the relative speed displacement change between the body and the wheels.

In evaluating the ride comfort and smoothness of a vehicle during driving, we pay more attention to the amplitude of the vertical displacement, the magnitude of the vertical velocity, and the change in the magnitude of the vertical acceleration of the spring-loaded part of the vehicle. Skyhook is to design and install an ideal skyhook damper between the vehicle body and the imaginary sky, which is essentially realized by suppressing the vertical velocity of the vehicle body. The controller acts through the relationship between the body sagging velocity and the suspension velocity relative to the body change velocity. Due to the addition of a magnetic force generator in the suspension system to provide a negative stiffness restoring force, it is possible that the dynamic travel of the suspension increases, and it takes a certain amount of time for the suspension velocity to change relative to the body change velocity, which makes the damping action behavior lag behind in time, and thus does not improve ride comfort. Improvement of ride comfort.

2.1. The Design of Negative Stiffness Model

We propose an improved skyhook control algorithm for the aforementioned negative stiffness suspension model with the main purpose of improving ride comfort. The improvement idea is to improve the relationship between the measured body droop speed and suspension speed relative to the body speed change into the relationship between the measured body droop speed and suspension droop speed on the original skyhook control strategy to achieve the purpose of suppressing vehicle vibration and improving vehicle ride comfort.

We model the quarter-vehicle negative stiffness suspension system shown in Figure 3 and formulate its dynamics equations:

$$\begin{cases} m_s\ddot{x}_s + g(x_s - x_u) + c_0(\dot{x}_s - \dot{x}_u) + F_d = 0 \\ m_u\ddot{x}_u - g(x_s - x_u) - c_0(\dot{x}_s - \dot{x}_u) + k_t(x_u - x_r) - F_d = 0 \end{cases} \tag{4}$$

The improved skyhook is similar to the skyhook. The main purpose is to suppress the vibration of the body. According to the previous article, we have established the suspension negative stiffness model in parallel with a set of magnetic generators in the suspension to provide a negative stiffness recovery force near the vibration equilibrium point. The negative stiffness recovery force can be designed at the model level itself. We design here the negative stiffness recovery force formula as follows:

$$g(Z) = k_0 + k_1 Z + k_2 Z^2 + k_3 Z^3 + k_4 Z^4 + k_5 Z^5 \tag{5}$$

where the one-dimensional coefficients of each subterm are: $k_0 = 4.57 \times 10^4$, $k_1 = -4.337 \times 10^4$, $k_2 = -2.318 \times 10^5$, $k_3 = 1.121 \times 10^7$, $k_4 = -4.741 \times 10^6$, $k_5 = -1.195 \times 10^8$.

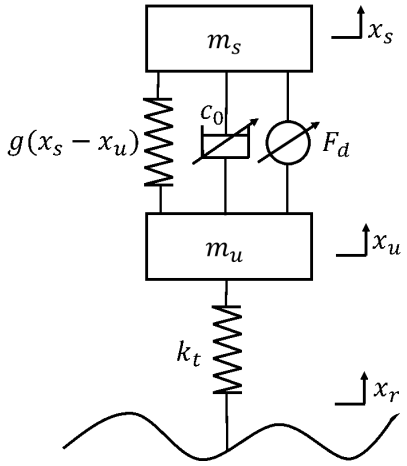

Figure 3. Improved sky and groundhook negative stiffness semi-active suspension.

Where the one-dimensional independent variable Z is the amount of deformation of the suspension, we first analyze this negative stiffness characteristic restoring force, for which the derivative is obtained as follows:

$$g'(Z) = k_1 + 2k_2Z + 3k_3Z^2 + 4k_4Z^3 + 5k_5Z^4 \tag{6}$$

Taking in the individual coefficients and making $g'(Z) = 0$ yield: $Z_1 = -0.2576$, $Z_2 = 0.2104$, $Z_3 = 0.0451$, $Z_4 = -0.0297$. According to the suspension travel design situation need to discard two absolute values of the larger value. In order to analyze the negative stiffness characteristics of the recovery force trend characteristics, we continue the derivative $g'(Z)$ and find the zero point can be obtained as follows: $Z_1 = -0.1832$, $Z_3 = 0.1524$. Combined with the image analysis, it can be obtained that when $Z \in (-0.1832, -0.0297]$, the stiffness of this suspension system decreases with the deformation because the deformation is negative at this time, and the absolute value of X becomes smaller, then the deformation of the suspension is also becoming smaller, for the process of shrinking after the suspension stretching, the process of the stiffness becomes smaller to enable the spring to better absorb the rebound energy. The suspension system exhibits negative stiffness characteristics when $Z \in (-0.0297, 0.0451)$. The overall suspension stiffness variation curve is shown in Figure 4.

The relationship between body droop speed and wheel droop speed is first analyzed in relation to Figure 5.

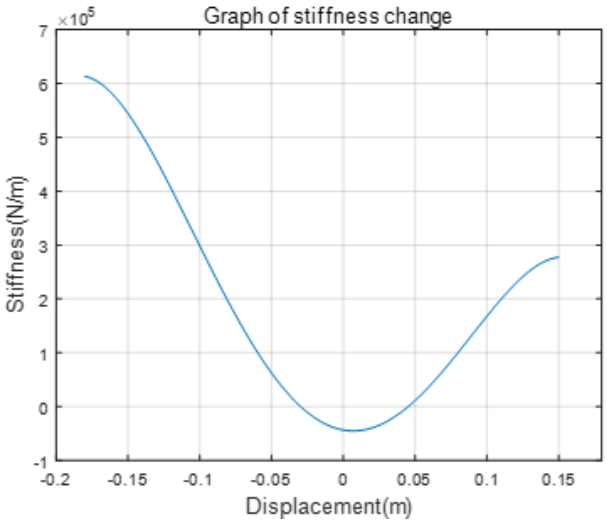

Figure 4. Stiffness variation curve.

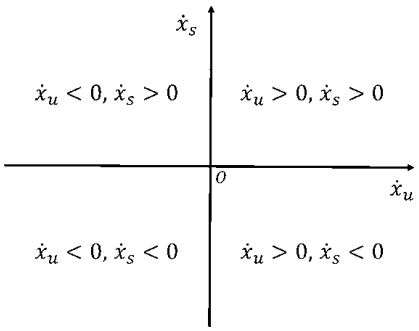

Figure 5. Body and wheel vertical velocity relationship.

According to Figure 5, we choose the suspension vibration equilibrium point as the origin, the direction on the orientation is positive, according to the body speed and wheel speed direction will be divided into four cases and corresponding to different quadrants. We can find that in the I and III quadrants of Figure 5, the body vertical velocity $\dot{x}_s$ and wheel vertical velocity $\dot{x}_u$ direction is the same As shown in Figure 6a,c, the body and wheels show the tendency of moving in the same direction at this time, which can be understood as the vehicle passing through the bumpy road or potholes, because there is already a negative stiffness characteristic restoring force to prompt the suspension to act during the vibration process, considering that the restoring force will increase the dynamic travel of the suspension, the speed change difference between the suspension and the body is reduced by increasing the coefficient of the damper. This can reduce the vibration transmitted by the suspension to the body, which can directly reduce the speed change in the body and the travel of the body.

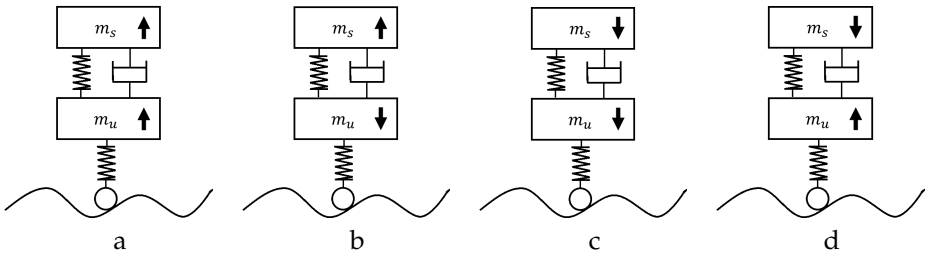

Figure 6. Schematic diagram of body and wheel vertical velocity. It illustrates four distinct types of relative relationships (**a**–**d**).

In quadrant II and III of Figure 5, the body droop velocity $\dot{x}_s$ and wheel droop velocity $\dot{x}_u$ are in opposite directions, as shown in Figure 6b,d, at this time the body and wheels show a tendency to move in the opposite direction, which we can understand as the backhaul situation when encountering a bumpy road or a potholed road, at which time the negative stiffness characteristic The restoring force is used to induce the suspension to act in the process of vibration contraction or extension, and because the force has travel-related characteristics, the speed change difference between the suspension and the body is reduced by decreasing the coefficient of the damper in the process of restoring to the initial equilibrium position, which can reduce the vibration brought to the body when the suspension returns to the original state, which can also directly reduce the speed change in the body. Considering that the algorithm is relatively simple, we will attribute the case of the presence of 0 to the first case.

Based on the above conclusions, we can design the control law for Equation (4). $F_d = c_d \dot{x}_s$ in Equation (4), where the control law for c_d is:

$$c_d = \begin{cases} c_{\min}, \dot{x}_u \dot{x}_s < 0 \\ c_{\max}, \dot{x}_u \dot{x}_s \geq 0 \end{cases} \tag{7}$$

Since it is difficult to obtain the analytical solution of this system of dynamics equations because the system contains higher-order terms about the dynamic travel of the suspension, we choose to perform numerical analysis in simulation to determine the performance of this suspension system.

2.2. Sky-Negative Controller Performance Simulation Analysis

We simulate and analyze this suspension system using random road signal, bump road signal and swept signal as input signals, respectively. Meanwhile, in order to analyze the performance of the suspension in a better and more intuitive way, we added passive suspension, negative stiffness suspension, and skyhook suspension for comparison. This paper focuses on vehicle body vibrations caused by road surface irregularities, with frequencies typically ranging from 0.1 Hz to 20 Hz at a speed of 72 km/h.

2.2.1. Sky-Negative Controller Performance Random Road Signal Simulation

Since the class skyhook control mainly targets the vibration suppression of the body, we only analyze some simulation data of the spring load part here. We can visually see from Figures 7–9 that the improved damping control strategy combined with the negative stiffness suspension can effectively attenuate the body vibration amplitude under the same random road input, while the velocity and acceleration of the body vibration are also effectively suppressed.

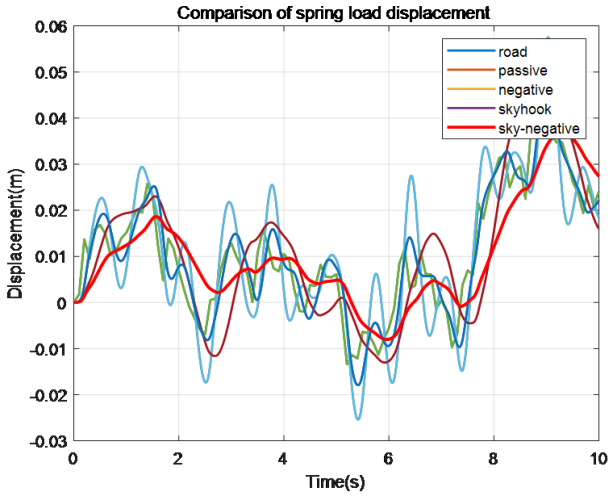

Figure 7. Spring load displacement comparison chart.

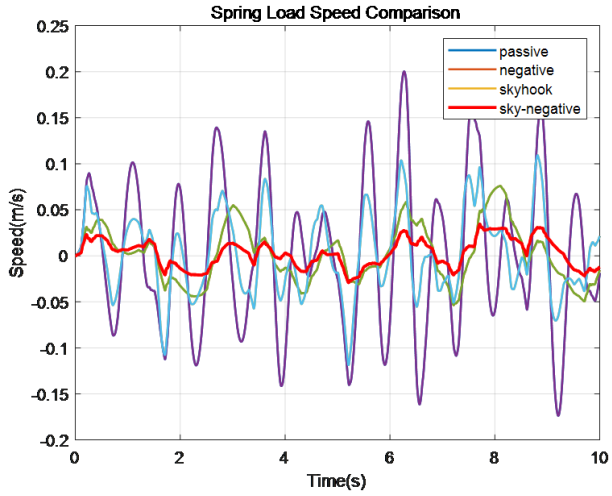

Figure 8. Comparison of spring load speed.

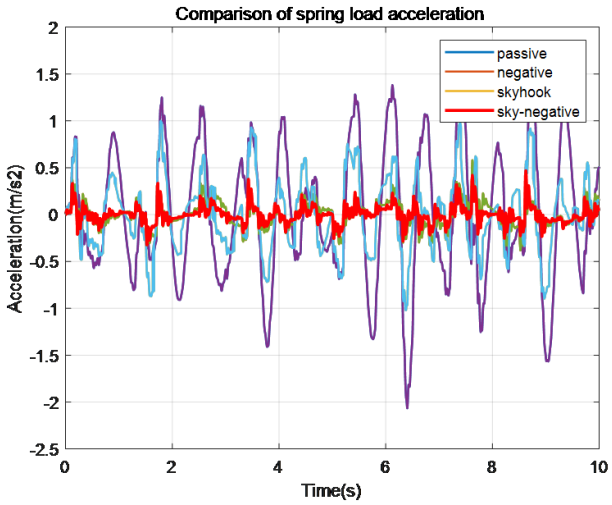

Figure 9. Comparison of spring load acceleration.

To enable quantitative analysis, we calculate the root mean square values of the body vibration amplitude response, body velocity response, and body acceleration response indicators and the degree of optimization calculated as shown in Table 1.

Table 1. Results of each index.

Methods	Displacement		Speed		Acceleration	
	RMS	Optimization	RMS	Optimization	RMS	Optimization
Passive	0.0154	——	0.0851	——	0.7157	——
Skyhook	0.0137	11.04%	0.0538	36.78%	0.4194	41.40%
Negative	0.0158	−2.60%	0.0303	64.39%	0.1534	78.57%
Sky-negative	0.011	28.57%	0.0157	81.55%	0.0942	86.84%

According to the data in Table 1, we can analyze and know that different suspension control methods and different characteristics of the suspension in the body vibration amplitude, body speed, and body acceleration suppression effect have their own characteristics.

In terms of body vibration amplitude suppression, compared to the passive suspension, the skyhook semi-active control suspension has an 11.04% improvement, the negative stiffness suspension has a slight deterioration of 2.60%, and the new improved damping control negative stiffness suspension has an improvement of 28.57%. In terms of body speed suppression, compared to the passive suspension, the skyhook semi-active control suspension has a 36.78% improvement, the negative stiffness suspension has a 64.39% improvement, and the new improved damping control negative stiffness suspension has an 81.55% improvement.

In terms of body acceleration suppression, compared to the passive suspension, the skyhook semi-active control suspension has a 41.40% improvement, the negative stiffness suspension has a 78.57% improvement, and the new improved damping-controlled negative stiffness suspension has an 86.84% improvement. It can be seen that under random road excitation, our proposed new improved damping-controlled negative stiffness suspension system has some or greater improvement compared to other suspension systems.

Since a set of magnetic generators is added to the suspension to provide negative stiffness characteristics, its suspension dynamic travel at the vibration balance point is bound to increase. In order to be able to quantitatively analyze the effect of the class skyhook control method on the suspension dynamic travel, we set up a comparison at the same suspension condition. We compared the effect of the control method on the normal suspension and the effect of the control method on the negative stiffness suspension, respectively.

From Figures 10 and 11, we can see that the skyhook control and class improved skyhook control have a great improvement compared to the passive suspension in the ordinary suspension dynamic travel comparison. In Table 2, we give the data of the root mean square value of the dynamic travel for comparison. The effect of skyhook control in the normal suspension is 35.44% higher than that of the passive suspension, and the effect of improved skyhook control is 29.11% higher than that of the passive suspension, and its control effect decreases compared to skyhook control but is within a certain control range. In the comparison of the dynamic travel of negative stiffness suspension, the dynamic travel of negative stiffness suspension is increased compared with that of passive suspension due to the special characteristics of its structure, but when the improved skyhook control is added, the dynamic travel of the suspension is optimized by 11.24% compared with that of the negative stiffness suspension.

Table 2. Various types of suspension dynamic travel indicators.

Methods	General		Methods	Negative Stiffness	
	RMS/10^{-4}	Optimization		RMS/10^{-4}	Optimization
Passive	79	——	negative	89	——
Skyhook	51	35.44%			
Groundhook	56	29.11%	new-negative	79	11.24%

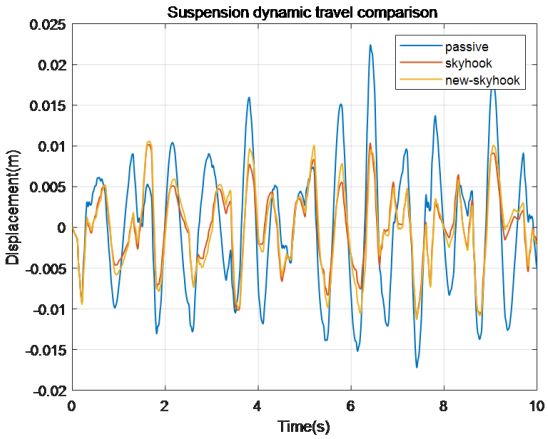

Figure 10. Comparison of spring load speed.

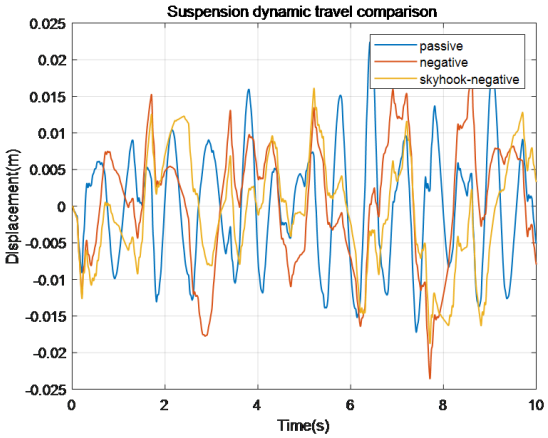

Figure 11. Comparison of spring load acceleration.

2.2.2. Sky-Negative Bump Pavement Signal Simulation

We changed the random input signal to a bumped road signal to simulate the performance of the suspension when going over a bumped road, such as a speed bump: Similarly,

we can visualize in Figures 12–14 that the vibration amplitude of the skyhook-like negative stiffness suspension is smaller than any other suspension system when passing over a bumpy road surface, and the vibration transmission amplitude is reduced by 13.6%, which has a non-negligible effect on the energy reduction transferred to the reeded mass portion by the road excitation; in the acceleration comparison performance of the skyhook-like negative stiffness suspension peak acceleration is smaller than any other method or suspension.

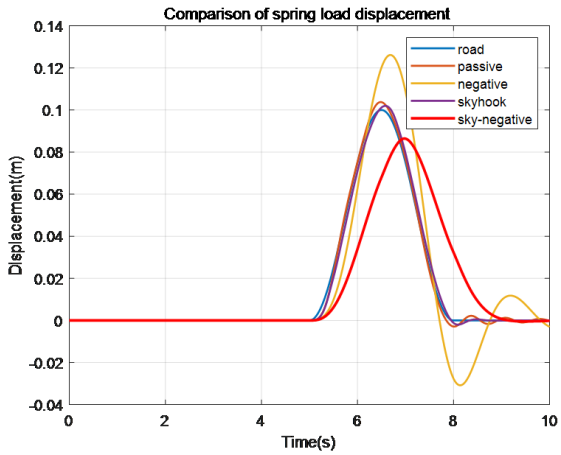

Figure 12. Comparison of spring load displacement.

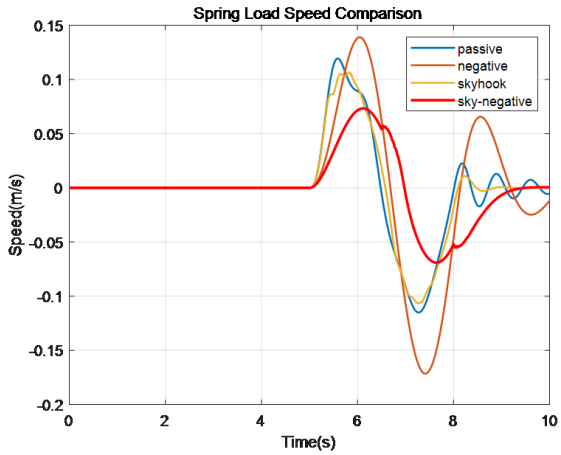

Figure 13. Comparison of spring load speed.

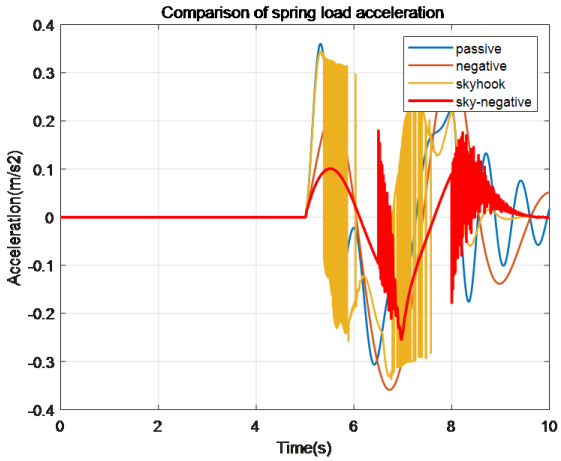

Figure 14. Comparison of spring load acceleration.

2.2.3. Sky-Negative Sweep Input Signal Simulation

Finally, we use the swept signal with the frequency range of 0∼18 Hz as the input signal to test the performance of the suspension, and the specific results are shown in Figure 15.

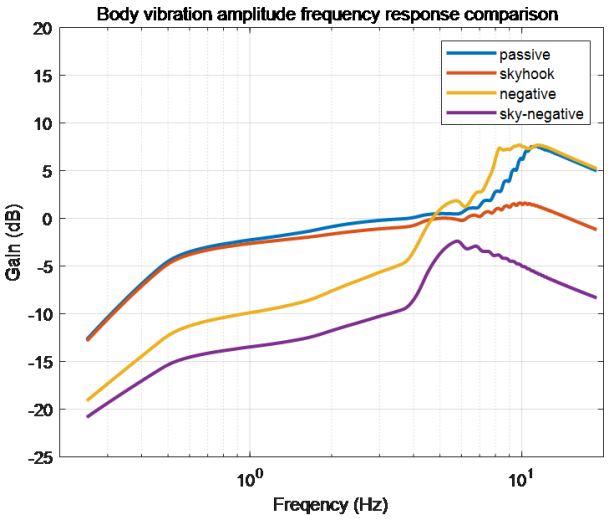

Figure 15. Comparison of frequency response of body vibration amplitude.

From Figure 15, we can see that in the set frequency range, the new, improved damping control negative stiffness suspension has a better effect on vibration suppression than all other suspension systems; among them, the passive control method and the skyhook control method have a similar effect in the low-frequency stage, the negative stiffness characteristic suspension has a better effect on vibration suppression than the first two, and the new, improved damping control negative stiffness suspension has the best control effect; however, in the middle-frequency range, the gain of the negative stiffness characteristic suspension and the new, improved damping control negative stiffness suspension has increased compared with the other two control methods. In the middle-frequency band, the gain of negative stiffness characteristic suspension and new, improved damping control negative stiffness suspension increases compared with the other two control methods, and the gain of negative stiffness characteristic suspension crosses and exceeds the passive control method and skyhook control method; in the high-frequency band, the gain of negative stiffness characteristic suspension is almost the same as that of passive suspension, and it is the highest among the four methods, while the gain of new, improved damping control negative stiffness suspension is still smaller than the other This shows that the control effect of the new, improved damping control negative stiffness suspension proposed in this paper is better than the other three suspensions in all frequency bands, and has better suppression performance for road excitation vibration.

2.3. Ground-Negative Controller Performance Simulation

Next, we simulate and verify the proposed new, improved groundhook control for negative stiffness suspension. Since the previously mentioned skyhook control method is a vibration suppression method for the spring load-displacement part, the new, improved groundhook control method on the negative stiffness suspension here is a vibration control method for the non-spring load-displacement part of the vehicle, and we focus on the analysis of the unsprung load-displacement part in the simulation.

2.3.1. Ground-Negative Controller Random Road Signal Performance Simulation

Figure 16 shows the unsprung load displacement of the newly improved groundhook-controlled negative stiffness suspension compared with several other methods.

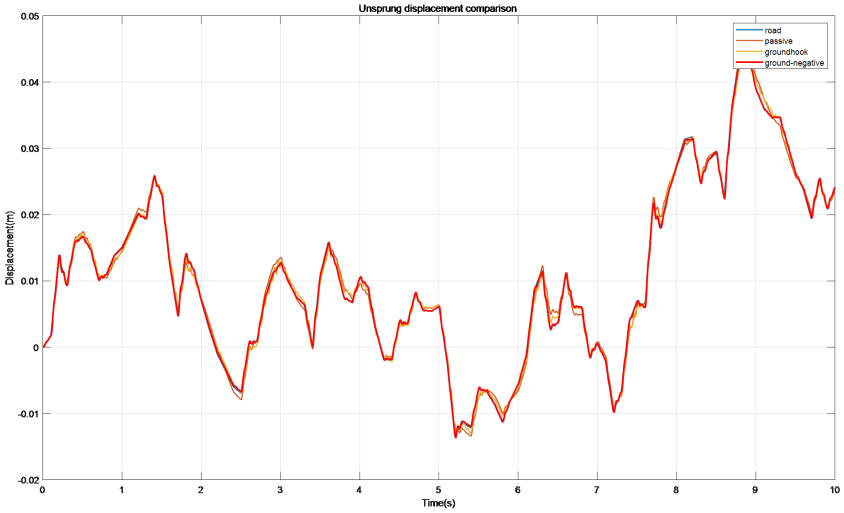

Figure 16. Comparison of unsprung load displacement of different control methods.

According to the enlarged picture, we can see that the control effect of the three methods is better when the road direction is smooth on a smaller time scale, but when encountering a sudden turn or continuous turn of the road, both the passive suspension and the groundhook control see their control error become larger. The vibration amplitude and frequency of these two methods, in turn, will also increase in the actual situation. The new, improved groundhook control negative stiffness suspension has the best tracking effect. It can track the road excitation signal well when encountering sudden or continuous turns, and it can maintain good smoothness and basically does not produce high-frequency vibration, which can effectively protect the structural performance of the suspension.

From Figure 17, it can be seen that the dynamic wheel deformation of the passive control suspension, the shed damping control suspension, and the new, improved groundhook control negative stiffness suspension can all be maintained within a certain range. Since the graph cannot accurately judge the effect of various methods, we calculate the root mean square values of the dynamic wheel deformation of the three methods as shown in Table 3.

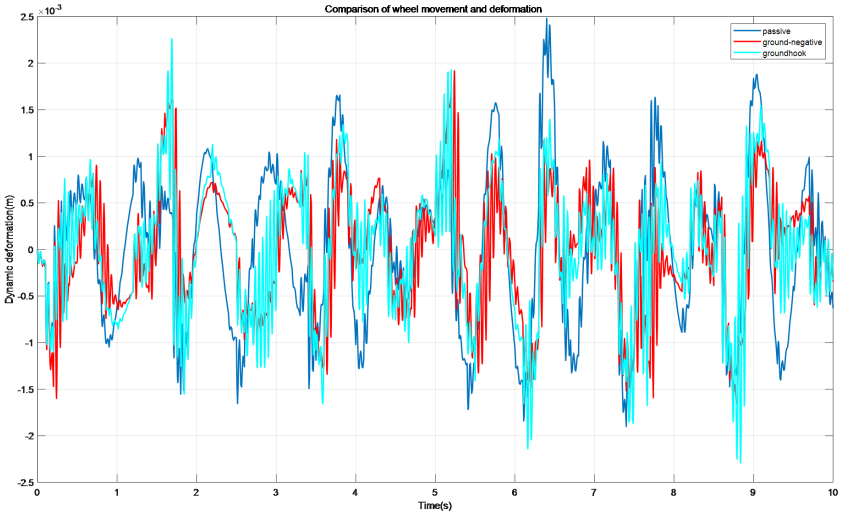

Figure 17. Comparison of wheel dynamic deformation by different control methods.

Table 3. Table of root mean square values of wheel dynamic deformation.

Methods	Passive	Groundhook	Gro-Negative
RMS/10^{-4}	7.90	7.70	7.61

From Table 3, it can be seen that the RMS value of wheel dynamic deformation for the passive control method is the largest, 7.8997; the RMS value of wheel dynamic deformation for the shed damping control is 7.6977, which is 2.56% less than the RMS value of wheel dynamic deformation for the passive control method; the RMS value of wheel dynamic deformation for the new, improved groundhook control negative stiffness suspension is 7.6139, which is 3.62% less than the RMS value of wheel dynamic deformation for the passive control method. The RMS value of wheel dynamic deformation for the new, improved groundhook control negative stiffness suspension is 7.6139, which is 3.62% less than that of the passive control method. It can be seen that the new improved shed-controlled negative stiffness suspension can also reduce the wheel dynamic deformation, so that the wheels can better fit the ground and enhance the grip performance of the wheels.

2.3.2. Ground-Negative Controller Bump Pavement Signal Simulation

The results are shown in Figures 18–20. Under the excitation of the bumped road, the peak vibration amplitude of the new, improved groundhook-controlled negative stiffness suspension is smaller than that of the other three suspension systems, and its tendency of rebound motion during the recovery process is smaller compared with that of the negative stiffness suspension so that the vibration amplitude and the number of vibrations during the recovery process are correspondingly smaller. The vibration amplitude and the number of vibrations will be correspondingly smaller, which can indirectly improve the vehicle ride comfort.

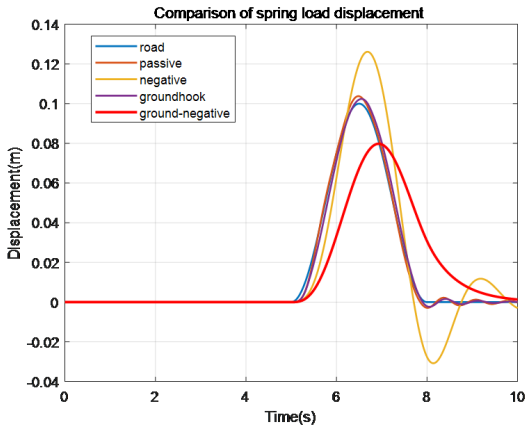

Figure 18. Comparison of spring load displacement.

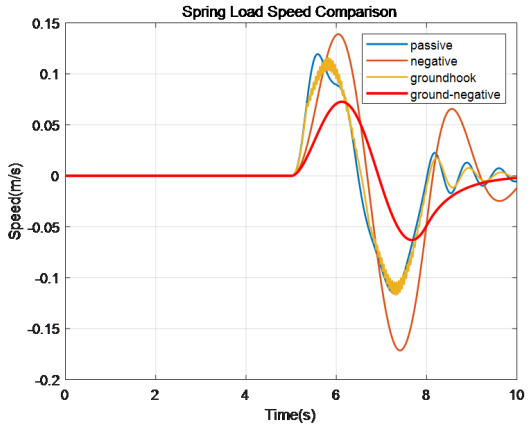

Figure 19. Comparison of spring load speed.

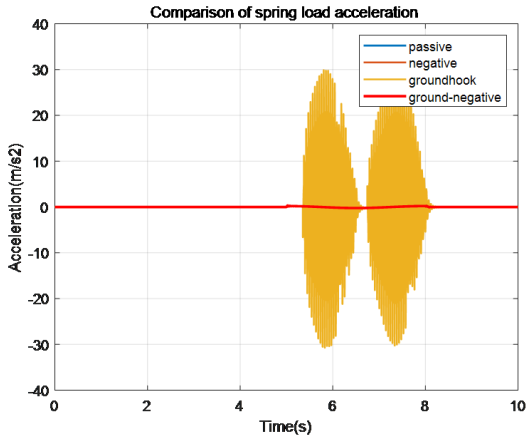

Figure 20. Comparison of spring load acceleration.

2.3.3. Ground-Negative Sweep Input Signal Simulation

We tested the frequency response of the suspension body part to the road sweep excitation signal in the frequency range of 0-18Hz, and the results are shown in Figure 21. From Figure 21, we can see that in the set frequency range, the effect of the new improved groundhook control negative stiffness suspension on vibration suppression is also better than all other suspension systems; among them, the passive control method and the groundhook control method have similar effects in the low-frequency stage, and the negative stiffness characteristic suspension has a better effect on vibration suppression than the first two, and the new improved groundhook control negative stiffness suspension has the best control effect; However, in the middle-frequency band, the gain of negative stiffness characteristic suspension and new improved groundhook control negative stiffness suspension has increased compared with the other two control methods, and the gain of negative stiffness characteristic suspension crosses and exceeds the passive control method and skyhook control method; in the high-frequency band, the gain of negative stiffness characteristic suspension is almost the same as that of passive suspension, which is the highest among the four methods, while the gain of new improved groundhook control negative stiffness suspension is still smaller than that of the other three suspensions. This shows that the control effect of the new, improved groundhook control negative stiffness suspension proposed in this paper is better than the other three suspensions in all frequency bands, and it also has better suppression performance for road excitation vibration.

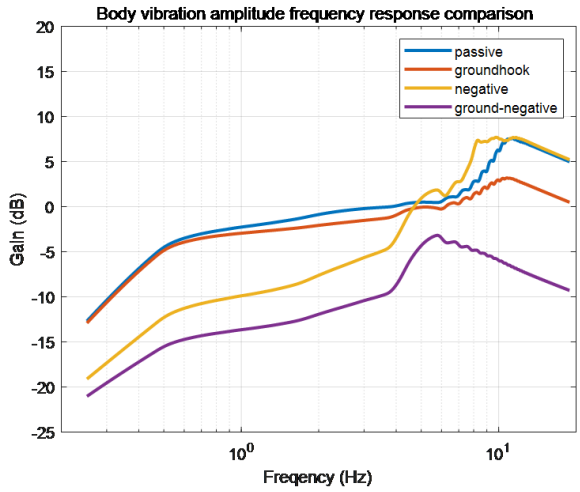

Figure 21. Comparison of frequency response of body vibration amplitude.

3. Design of Hybrid Control Algorithm for Negative Stiffness Semi-Active Suspension

In the previous section, an improved shed-like control method was designed and simulated by analyzing and verifying the sky and groundhook control methods and combining the dynamics of the controlled object. In this chapter, the advantages of the two control methods in the previous paper are combined to design and simulate a hybrid controller for negative stiffness semi-active suspension.

3.1. Semi-Active Suspension Hybrid Control Algorithm

There is a class of hybrid control algorithms derived from the sky skyhook, of which the more representative one is the hybrid skyhook-acceleration damping-driven semi-active control algorithm (SH-ADD). Numerous analyses have shown that the skyhook control strategy provides the best control effect in the low-frequency band, while the acceleration-driven damping control provides a better control effect in the middle and high-frequency bands, and these two control strategies complement each other in the full-frequency band. The control idea of the hybrid skyhook-acceleration damping-driven semi-active control algorithm is to use a very simple and effective frequency band selector to identify the current motion characteristics of the suspension and to select the skyhook control strategy in the low-frequency phase and switch to acceleration damping-driven semi-active control in the mid–high-frequency phase. The hybrid control law proposed by this method is as follows:

$$c_{in} = \begin{cases} c_{\max}, \left[(\ddot{x}_s^2 - \alpha^2 \dot{x}_s^2) \le 0 \quad and \quad \dot{x}_s(\dot{x}_s - \dot{x}_u) > 0\right] \\ \quad or \left[(\ddot{x}_s^2 - \alpha^2 \dot{x}_s^2) > 0 \quad and \quad \dot{x}_s(\dot{x}_s - \dot{x}_u) > 0\right] \\ c_{\min}, \quad others \end{cases} \tag{8}$$

where: $c_{\max}$ and $c_{\min}$ are the maximum and minimum values of the damping coefficient, respectively, and $\{c_{\max}, c_{\min}\} \in \mathbb{R}^+$ and $\alpha \in \mathbb{R}^+$. The method actually establishes a static observation strategy to achieve the control of the damping coefficient, and it uses only three parameters, $\ddot{x}_s$, $\dot{x}_s$ and $\dot{x}_u$, in the control process. The velocity of the vehicle can be obtained by integrating the measured acceleration values, and the velocity of the unsprung part can also be measured and calculated by installing an accelerometer on the wheel structure.

During the control process, Equation (8) will select a different control strategy depending on the current value of $\ddot{x}_s^2 - \alpha^2 \dot{x}_s^2$. If $\ddot{x}_s^2 - \alpha^2 \dot{x}_s^2 > 0$, the acceleration-driven damping control strategy is selected, and at other moments, the skyhook control strategy is selected.

The value of $\ddot{x}_s^2 - \alpha^2 \dot{x}_s^2$ can be considered to be a simple "band selector" according to the above, where the parameter α represents the switching frequency referred to when the "selector" selects a different frequency band. It is the only adjustable parameter in this selection reference strategy. The parameter can be determined by calculating the crossover frequency between the skyhook control algorithm and the acceleration-driven damping control algorithm, and a typical standard motorcycle suspension α value is set to about 19 rad/s, so the switching frequency is set at about 3 Hz. However, the specific switching parameter α must be determined according to the specific situation and parameters of the suspension.

3.2. Design of Hybrid Controller for Negative Stiffness Semi-Active Suspension

In the suspension system that does not have negative stiffness during operation, there are many control algorithms to optimize the performance for different aspects of various types of suspensions, but for the new type of suspension system introduced in this paper that has stroke-related negative stiffness characteristics, the existing control algorithms cannot achieve a better control effect on this suspension. In the previous chapter, we designed skyhook-like and groundhook-like control algorithms, respectively, and simulated and analyzed these two methods. It can be seen that, for the front suspension system, the skyhook-like control algorithm is better than the groundhook-like control algorithm in suppressing the body vibration; however, its performance in the control of wheel dynamic deformation is not as good as the groundhook-like control algorithm, so we

combine the advantages of the two control strategies with each other and design the new semi-active negative stiffness hybrid control algorithm for this suspension. We combine the advantages of the two control strategies to design a new semi-active negative stiffness hybrid suspension control algorithm. In the skyhook-like control algorithm, we select the damping in the suspension semi-active control method according to the product of the vibration velocity of the spring-loaded mass and the vibration velocity of the unsprung mass. When the product of the velocity of the spring-loaded mass and the velocity of the unsprung mass part is less than zero, a smaller damping coefficient is selected in the strategy, and vice versa, a larger damping coefficient is selected. In the groundhook-like control algorithm, we are based on the relationship between the product of the unsprung mass vibration velocity and the wheel vibration velocity to choose to damp in the semi-active control method of the suspension when the product of the sprung mass velocity and the wheel vibration velocity is less than zero, the strategy selects smaller damping coefficients, and vice versa, selects larger damping coefficients. Then, to combine the advantages of both, it is necessary to select the damping in the suspension semi-active control algorithm according to the three parameters: the speed of the vibration of the spring-loaded mass, the speed of the vibration of the unsprung mass, and the speed of the vibration of the wheel. Based on this analysis, when the product of the spring-loaded mass velocity and the unsprung mass velocity is negative and the product of the spring-loaded mass velocity and the wheel vibration velocity is also negative, the system state aligns with the skyhook criteria. In this scenario, selecting a lower damping coefficient for the skyhook control method will result in better control. In other cases, where the product of these two parameters is positive, it is recommended to choose a higher damping value to ensure optimal system control.

The designed control strategy is as follows:

$$c_d = \begin{cases} c_{\min}, \dot{x}_r \dot{x}_u < 0 \, and \, \dot{x}_s \dot{x}_u < 0 \\ c_{\max}, others \end{cases} \tag{9}$$

where c_d is the damping factor of the system input, $c_{\max}$ is the maximum damping value that the system can provide, and $c_{\min}$ is the minimum damping value designed by considering the damping characteristics of the system.

3.3. Simulation Analysis of Controller Performance

We simulate this suspension system using random road signal, bump road signal and swept signal as the input signals, respectively. Meanwhile, in order to better and more intuitively analyze the performance of the suspension, we added passive suspension, negative stiffness suspension, skyhook suspension, and the class sky and floor skyhook negative stiffness semi-active suspension designed in the previous paper for comparative analysis. Due to the large number of comparison methods, we divided into two groups for comparison. The first group is passive control, skyhook control, and groundhook control, and the other group is negative stiffness suspension, improved skyhook control, and improved groundhook control.

3.3.1. Random Road Signal Simulation

First, we use the random road signal as the input signal for simulation analysis. From the simulation results in Figure 22, we can see that the vibration suppression effect of the hybrid control algorithm control on the spring load part is significantly better than that of the passive suspension and the traditional sky and groundhook control algorithm; and compared with the suspension control algorithm that adds the concept of negative stiffness, its vibration suppression effect on the spring load part is also better than that of the negative stiffness suspension and the negative stiffness control algorithm of the class sky and groundhook.

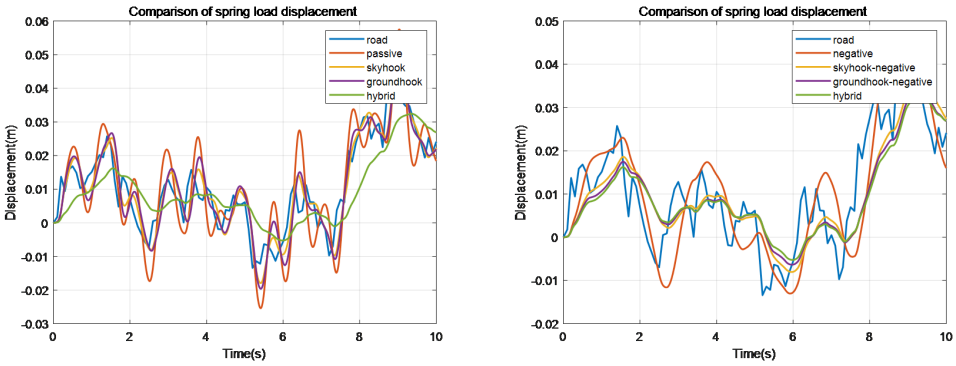

(**a**) (**b**)

Figure 22. Comparison of spring load displacement of different control methods. (**a**) Represents the original method, while (**b**) represents the negative stiffness method.

For the unsprung part, we intercepted the more representative parts of the simulation result image for enlargement, and in the enlarged part of the comparison Figure 23, we can clearly see that the tracking of the input road signal in the suspension part under the hybrid control method is more compact, especially at the moment when the road turns more, the tracking of the road by the suspension under the traditional passive suspension, skyhook and groundhook control algorithm will have certain error, in the negative stiffness suspension, the tracking effect of the hybrid control method on the road surface input signal is also to have some advantage over the tracking effect of the class sky and groundhook control method and the negative stiffness suspension. Although the difference in the figure is not very obvious, we have made the simulation data more accurate for comparison, and the specific numerical performance is shown in Table 4.

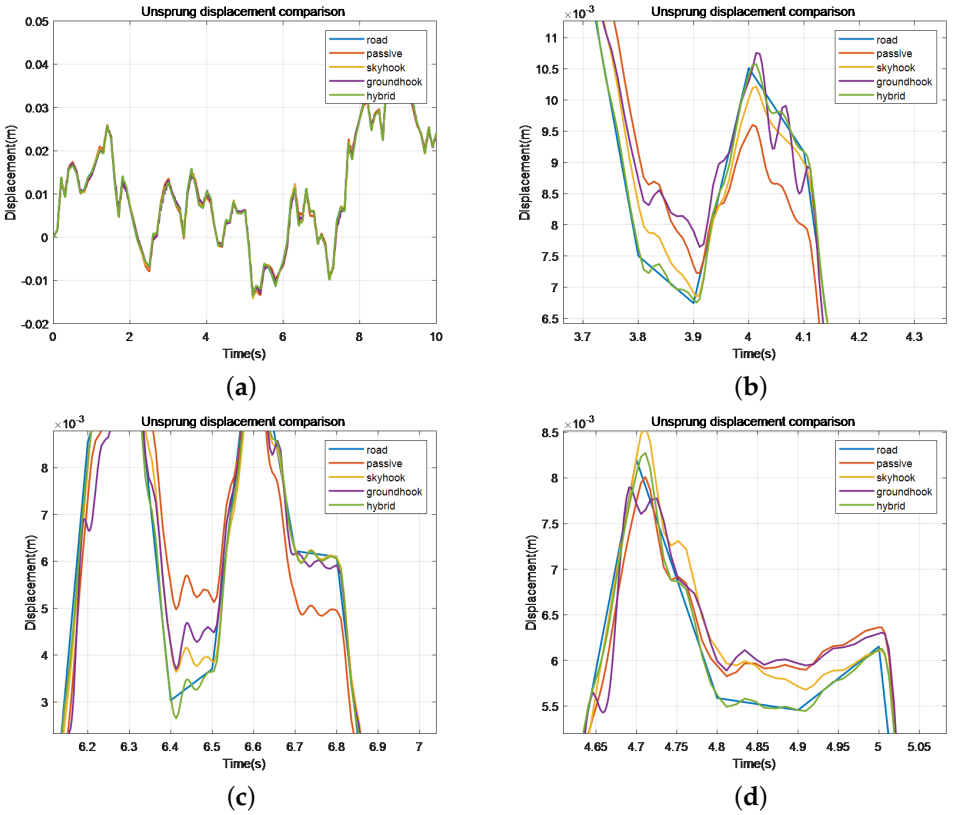

(**a**) (**b**)

(**c**) (**d**)

Figure 23. *Cont*.

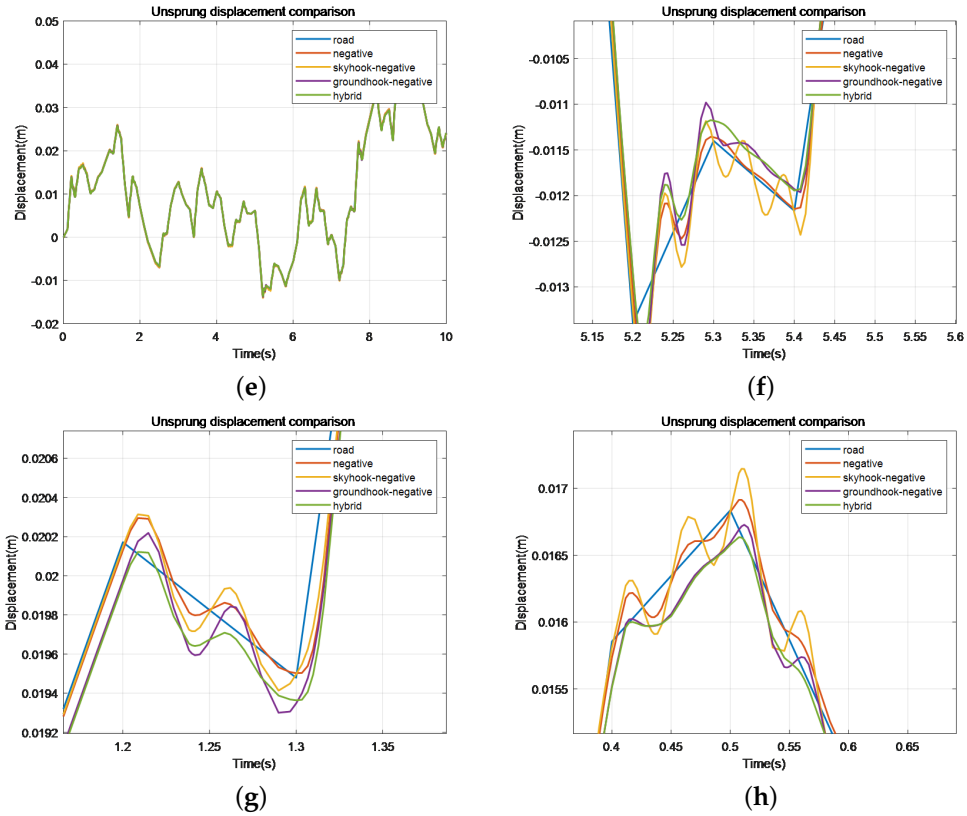

Figure 23. Enlarge part. Figures (**b**–**d**) are magnified views of specific regions within (**a**). Figures (**f**–**h**) are magnified views of specific regions within (**e**).

In terms of vibration suppression of the spring load section, the traditional skyhook control and groundhook control are effective, but the improvement is only 10% and 8%, respectively. However, the vibration suppression effect is significantly improved by adding the Sky and Groundhook control algorithm and the Hybrid control algorithm, which are 28.57%, 35.06% and 38.96%, respectively, which can also indirectly improve the smoothness of the vehicle. In the unsprung part, the effect of the hybrid control algorithm is similar to that of the shed and shed-like negative stiffness. Although the numerical change is small, when combined with the images, it can be found that the unsprung displacement performance of the hybrid negative stiffness control is the best among all methods.

Table 4. Comparison of spring-loaded and unsprung displacement values.

Methods	Spring Load Displacement		Unsprung Displacement	
	RMS	Optimization	RMS	Optimization
Passive	0.02	——	0.01	——
Skyhook	0.01	10.39%	0.01	0.0000%
Groundhook	0.01	7.79%	0.01	0.74%
Negative	0.02	−2.60%	0.01	0.00%
S-Negative	0.01	28.57%	0.01	0.74%
G-Negative	0.01	35.06%	0.01	0.00%
Hybrid	0.01	38.96%	0.01	0.74%

We also performed the image and numerical analysis for the spring-loaded and unsprung speeds, as shown in Figure 24, in terms of the control effect of the passive suspension as a comparison for the spring-loaded part of the speed, the skyhook control and the groundhook control improved by 35.25% and 31.49%, respectively, and when the negative stiffness feature was added, its control effect improved by 64.27% without any

control algorithm, and when the class sky and floor shed were added again and hybrid control algorithms, the control effect is improved by 81.2%, 82.49% and 83.78%, respectively. As shown in Figure 25, in terms of unsprung speed, in order to track the road input signal well and accurately in time, faster speed is needed to reduce the tracking error, and the performance under hybrid control can also be kept within a smaller disadvantage with other methods.

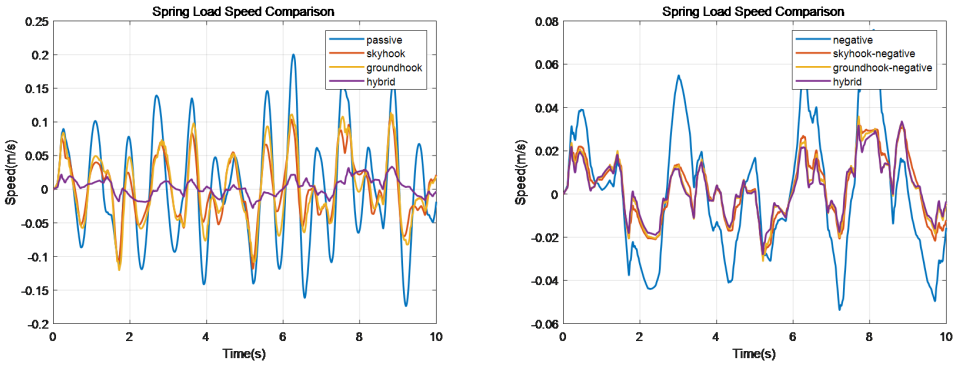

(**a**) (**b**)

Figure 24. Comparison of spring load speed of different control methods. (**a**) Represents the original method, while (**b**) represents the negative stiffness method.

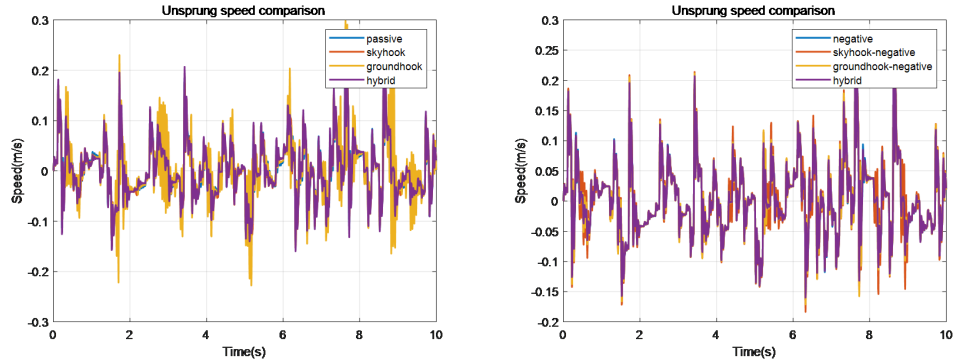

(**a**) (**b**)

Figure 25. Comparison of different control methods for unsprung load speed. (**a**) Represents the original method, while (**b**) represents the negative stiffness method.

In terms of acceleration, the acceleration of the spring-loaded mass part can most affect the ride experience of the driver and passenger. When the vehicle passes over a bumpy road, the vibration caused by the road is transmitted to the body through the suspension and then transferred from the body to the human body, so the acceleration of the body part is required to be as small as possible, so that the vibration felt by the human body will be reduced. In Figure 26 and Table 5, we can see that the control effect of hybrid control negative stiffness is the best regardless of the range of change or the peak of change, and it is comparable to the control effect of class skyhook negative stiffness. In the control effect compared with the passive suspension control, the skyhook control and floor skyhook control improve 41% and 35%, respectively, and the control effect of negative stiffness suspension improves 78.39%, and the effect improves 86.83% and 85.19% after adding the class skyhook and floor skyhook control, while the hybrid control effect improves 86.83%, which is comparable to the class skyhook control effect.

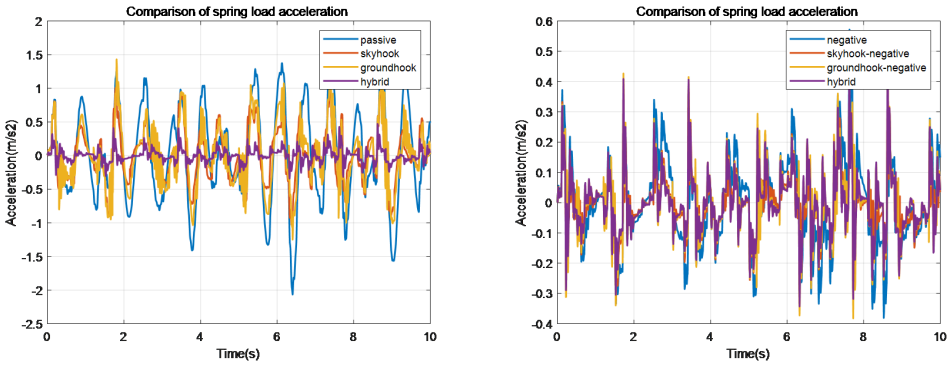

(**a**) (**b**)

Figure 26. Comparison of spring load acceleration of different control methods. (**a**) Represents the original method, while (**b**) represents the negative stiffness method.

Table 5. Comparison of spring-loaded and unsprung speed values.

Methods	Spring Load Speed		Unsprung Speed	
	RMS	Optimization	RMS	Optimization
Passive	0.09	——	0.06	——
Skyhook	0.05	35.25%	0.06	4.22%
Groundhook	0.05	31.49%	0.06	11.07%
Negative	0.03	64.28%	0.05	1.93%
S-Negative	0.016	81.19%	0.06	5.27%
G-Negative	0.01	82.49%	0.05	1.58%
Hybrid	0.01	83.78%	0.05	0.17%

In Figure 27, in the acceleration control performance of the unsprung mass part, as the performance of the hybrid control method in the displacement part of the unsprung mass is already the best among several control methods, then at this time to consider the impact of the acceleration size on the suspension, the smaller the acceleration is, the smaller the force on the suspension, which can not only maintain a better fit with the ground when passing over bumpy roads but also reduce the Acceleration to reduce the mechanical vibration consumption of the suspension, then Table 6 can clearly compare the hybrid control algorithm at this time in several control methods in the value of the performance is also in the forefront.

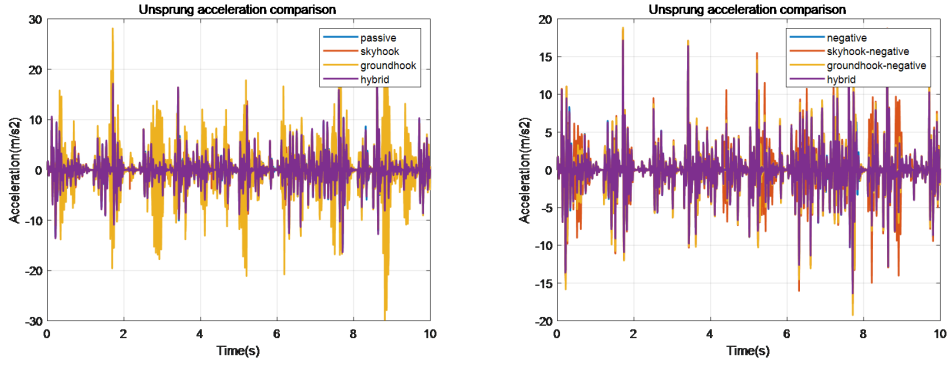

(**a**) (**b**)

Figure 27. Comparison of unsprung acceleration of different control methods. (**a**) Represents the original method, while (**b**) represents the negative stiffness method.

Table 6. Comparison of spring load acceleration and unsprung load acceleration values.

Methods	Spring Load Acceleration		Unsprung Acceleration	
	RMS	Optimization	RMS	Optimization
Passive	0.72	——	3.02	——
Skyhook	0.42	41.00%	2.97	−1.83%
Groundhook	0.46	35.33%	6.30	108.53%
Negative	0.15	78.39%	3.14	4.02%
S-Negative	0.09	86.83%	3.66	21.01%
G-Negative	0.11	85.19%	3.24	7.17%
Hybrid	0.09	86.83%	3.06	1.10%

In Figure 28, the performance in terms of suspension dynamic travel, due to the negative stiffness characteristic of the negative stiffness suspension, which exerts a force in the same direction as the wheel motion at the suspension equilibrium point, which can lead to an increase in suspension dynamic travel, after adding the class sky, floor shed and hybrid control, the three control methods are optimized by 11.83%, 13.93% and 12.90%. In Figure 29 and Table 7, in the performance of wheel dynamic deformation, with the wheel dynamic deformation of the passively controlled suspension as a reference, the skyhook control and the groundhook control are optimized by 40.13% and 0.8560%, respectively, and when the negative stiffness feature is added, the value of wheel dynamic deformation is greatly reduced and optimized by 69.87%, 65.29% and 66.01% under the class sky and groundhook control and hybrid control, respectively. With a greater reduction in wheel deformation, the degree of wheel-ground fit is increased to a greater extent, which increases the wheel grip capability and thus can increase the handling and safety of vehicle driving.

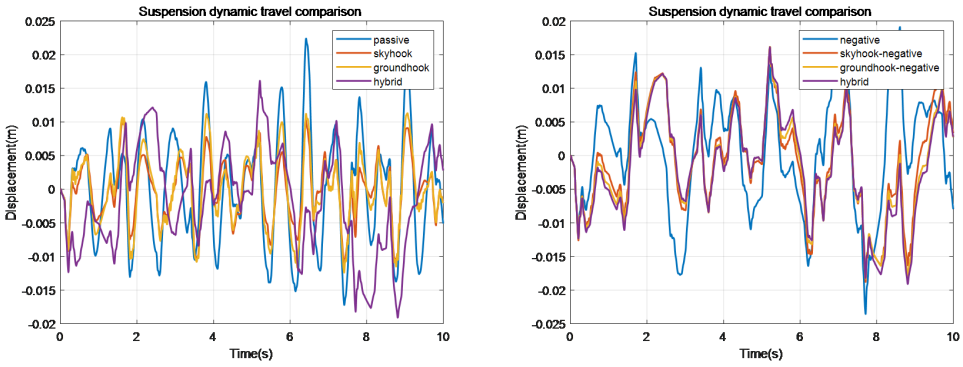

(**a**) (**b**)

Figure 28. Comparison of suspension dynamic travel by different control methods. (**a**) Represents the original method, while (**b**) represents the negative stiffness method.

Table 7. Comparison of the control effects of various control methods of suspension dynamic travel and wheel dynamic deformation.

Methods	Suspension Dynamic Travel		Wheel Movement Deformation	
	RMS/10^{-4}	Optimization	RMS/10^{-4}	Optimization
Passive	82	——	8.34	——
Skyhook	54	34.15%	4.99	40.13%
Groundhook	61	25.61%	8.27	0.86%
Negative	93	−13.41%	2.54	69.59%
S-Negative	82	0.00%	2.51	69.87%
G-Negative	80	2.44%	2.89	65.29%
Hybrid	81	1.22%	2.83	66.01%

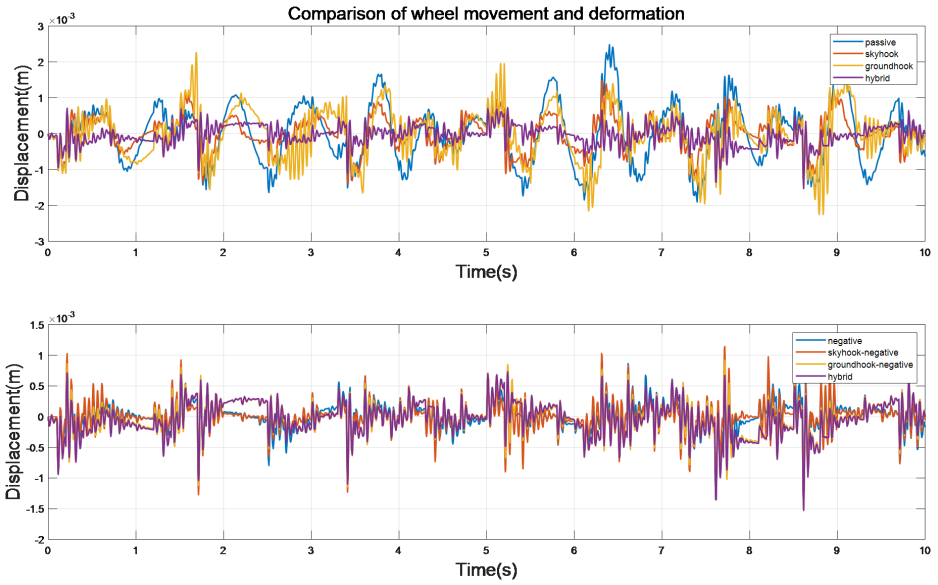

Figure 29. Comparison of wheel dynamic deformation by different control methods.

3.3.2. Bump Pavement Signal Simulation

We also needed to test the performance of the vehicle suspension system over potholes or bumps under the hybrid control method, and the results are shown below.

In Figure 30, when the vehicle passes over a bumpy road, less vibration amplitude is required to ensure the smoothness of the body during the driving process, and the test results show that the hybrid control has better suppression of the body vibration amplitude than other control methods in both the first and second group comparisons. The recovery process after the bumped road surface is short and gentle, and no continuous vibration occurs.

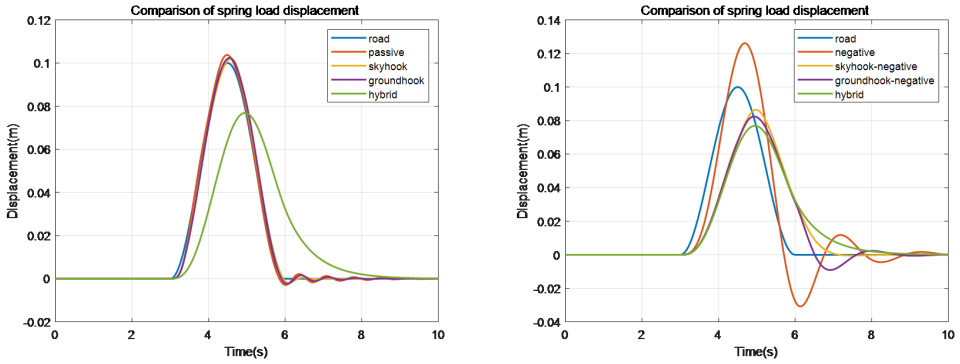

(**a**) (**b**)

Figure 30. Comparison of spring load displacement of different control methods. (**a**) Represents the original method, while (**b**) represents the negative stiffness method.

In Figures 31–35, the performance of the unsprung displacement shows that the groundhook control, skyhook-like control, and floor shed-like control all produce vibrations during passing over the bumpy road surface, which will accelerate the tire wear, while the suspension under the hybrid control is able to maintain a smoother tracking effect throughout passing over the bumpy road surface.

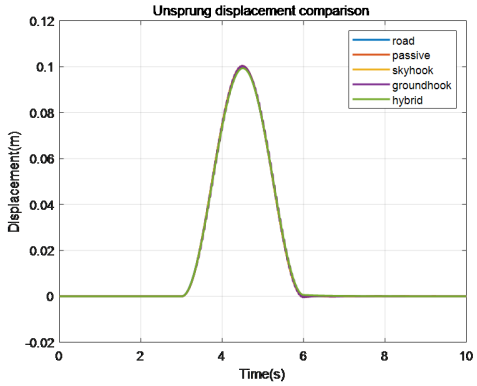

Figure 31. Comparison of unsprung load displacement of different control methods I.

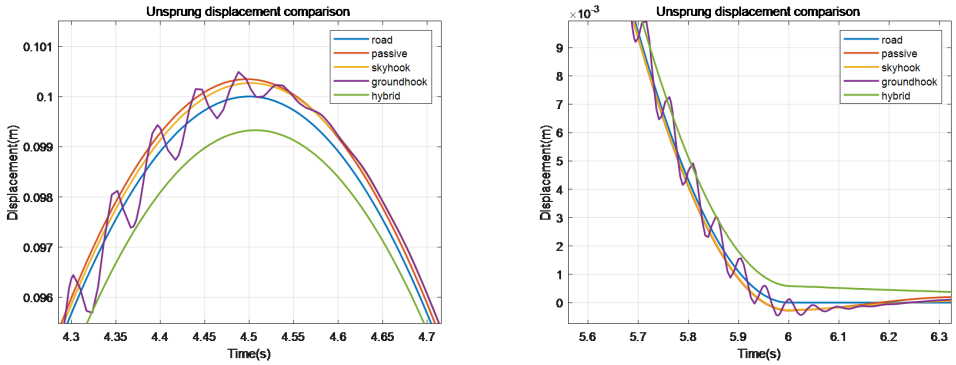

(**a**) (**b**)

Figure 32. Comparison of spring load displacement of different control methods about local dynamic plot (**a**,**b**).

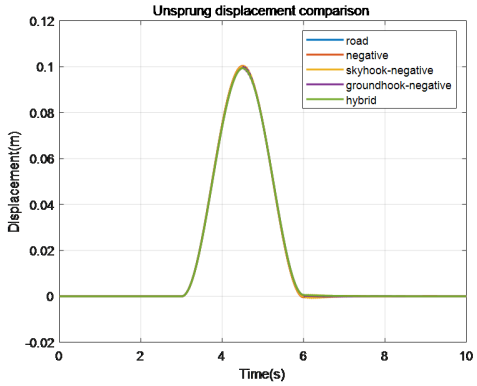

Figure 33. Comparison of unsprung load displacement of different control methods II.

The most intuitive feeling of the vehicle passing over the bumpy road is that the body is pushed upward, and as mentioned in the previous article, in order to ensure the smoothness of the body during driving, the smaller the vibration amplitude of the body is, the better. There is no continuous vibration. In Table 8, compared with the passive suspension control, the root mean square value of the acceleration of the hybrid control is reduced by 31.77%, which is the best among all control methods in this paper, and it can greatly improve the ride comfort of the vehicle when passing over bumpy roads such as speed bumps. In terms of wheel acceleration, the hybrid control algorithm has been introduced in the previous paper, the displacement tracking effect is relatively smooth and soft, and its tracking error can be compared and analyzed according to the dynamic wheel deformation.

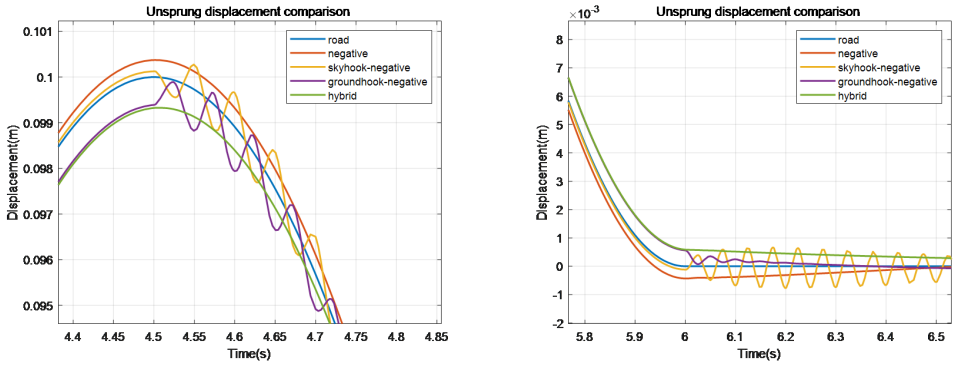

(**a**) (**b**)

Figure 34. Comparison of spring load displacement of different control methods about local dynamic plot (**a**,**b**).

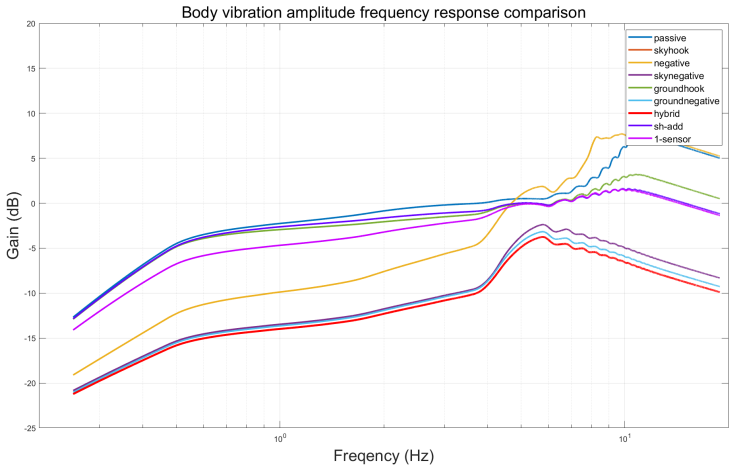

Figure 35. Comparison of frequency response of body vibration amplitude.

Table 8. Spring-loaded and unsprung acceleration indicators for various methods.

Methods	Spring Load Acceleration		Unsprung Acceleration	
	RMS	Degree of Change	RMS	Degree of Change
Passive	0.13	——	0.09	——
Skyhook	0.24	−84.62%	3.46	−3487.90%
Groundhook	0.45	−246.23%	14.45	−14,839.50%
Negative	0.20	−52.76%	0.09	−0.10%
S-Negative	0.12	11.00%	1.55	−1500.73%
G-Negative	0.10	19.84%	0.89	−824.61%
Hybrid	0.90	31.77%	0.09	1.45%

3.3.3. Sweep Input Signal Simulation

Finally, we conducted a frequency domain analysis of the system and simulated it by sweeping the signal with the input frequency range from 0 to 18 Hz. The negative stiffness-based hybrid control algorithm has the best suppression effect on the body regardless of the low-frequency or high-frequency part. The single-sensor algorithm, among other methods, can be better suppressed at low and medium frequencies, and the acceleration damping drive method is not as good as the negative stiffness hybrid control method. The frequency domain characteristics of the skyhook-like and floor-like control algorithms have been analyzed in the previous paper, so we will not repeat them here.

4. Discussion

The suspension system is critical for vehicle stability and ride comfort, as it supports the vehicle's weight while mitigating vibrations caused by uneven road surfaces. Semi-active suspension, offering a balance between cost-effectiveness and performance, has become the dominant technology in the market. Recent research introduced negative stiffness suspension, incorporating permanent magnets to enhance vibration suppression. Building on this innovation, our study investigated semi-active negative stiffness suspension systems. We analyzed the system dynamics, defining key concepts and performance metrics. We then refined traditional skyhook and groundhook control methods to better suit negative stiffness applications, demonstrating improved performance through simulations. Finally, we designed and simulated a hybrid controller combining the strengths of the improved skyhook control strategies, further enhancing ride comfort. This research aims to contribute to the development of more comfortable and efficient vehicles by advancing the understanding and application of negative stiffness suspension systems. Details of the discussion are as follows:

(1) This study investigated the effectiveness of a new class of skyhook negative stiffness semi-active suspension controller in mitigating vehicle body vibrations. Our analysis reveals significant improvements in ride comfort compared to both passive and traditional semi-active suspension systems. Compared to passive suspension, the new skyhook negative stiffness controller demonstrated a notable reduction in body vibration, achieving a 28.57% decrease in vibration amplitude and an 86.84% reduction in vibration acceleration. Furthermore, the controller optimized suspension dynamic travel by 11.24% compared to a passive negative stiffness suspension. When traversing bumpy roads, the new controller effectively reduced vibration peaks by 13.6%. The new skyhook negative stiffness controller consistently outperformed passive, skyhook, and negative stiffness-controlled suspensions in suppressing body vibrations across the full-frequency spectrum.

(2) Simulation results demonstrate the effectiveness of the proposed hybrid controller. Compared to the new class of skyhook negative stiffness semi-active controller, the hybrid controller achieved a significant improvement in ride comfort. Notably, it exhibited an 82.83% reduction in body acceleration on random roads and over 20% suppression 624 of vibration peaks on bumpy roads. Furthermore, the hybrid controller demonstrated smoother performance with reduced chatter and acceleration, leading to less wheel loss. These positive results extend across the full-frequency range, surpassing the performance of other control algorithms presented in this paper across all frequency bands. The innovation of this research work is to design a skyhook-like control method, a groundhook-like control method, and a hybrid control method for the negative stiffness suspension system, which can provide significant control effects for the negative stiffness suspension system and are applicable to different practical needs.

(3) Beyond body vibration suppression, the new controller also exhibited advantages in wheel deformation and grip performance. Compared to passive and traditional skyhook control, the new controller demonstrated a reduction in dynamic wheel deformation, enhancing grip and stability. While the new skyhook negative stiffness controller shows significant promise, further research is needed to explore the potential of hybrid control strategies that combine this approach with other advanced control techniques. This could lead to even more significant improvements in ride comfort and overall vehicle performance. In particular, we focus on the following: investigating the effect of different negative stiffness configurations on vehicle performance, developing robust control algorithms for real-world applications, including road disturbances, vehicle dynamics, and sensor noise, and examining the cost-effectiveness of negative stiffness suspension systems compared to conventional approaches.

In summary, this work has made a useful exploration of the vibration suppression of negative stiffness suspension systems and laid a good foundation for further in-depth research on negative stiffness suspension vibration isolation systems.

5. Conclusions

In conclusion, this research delves into the optimization of semi-active negative stiffness suspension systems, highlighting their potential to enhance vehicle ride comfort and handling. The study begins by analyzing the concept of negative stiffness and establishing performance evaluation indexes for the suspension system. Building upon traditional skyhook and groundhook control strategies, the research proposes novel control algorithms specifically tailored for negative stiffness suspension systems. Simulation results demonstrate the optimized performance of these new control methods compared to existing approaches. Furthermore, a hybrid controller combining the advantages of the new skyhook and groundhook control is designed and simulated. The findings of this research offer valuable insights into the design and control of semi-active negative stiffness suspension systems, paving the way for future advancements in vehicle ride comfort and handling.

Author Contributions: Conceptualization, Y.C., S.S. and Z.L. (Zhibin Li); methodology, Y.C.; software, Z.H.; validation, Y.C., Z.H. and S.S.; formal analysis, Y.C.; investigation, Z.H.; resources, Z.L. (Zhijie Li); data curation, S.S. and Z.H.; writing—original draft preparation, Z.H., Y.C. and Z.L. (Zhijie Li); writing—review and editing, S.S. and Z.L. (Zhijie Li); visualization, Z.H.; supervision, S.S. and Z.L. (Zhibin Li); project administration, S.S.; funding acquisition, S.S. and Z.L. (Zhibin Li). All authors have read and agreed to the published version of the manuscript.

Funding: This research was funded by the National Natural Science Foundation of China, Grant/Award Numbers: U23A20336, 61333008, 61603320.

Data Availability Statement: The data that support the findings of this paper are available from the authors upon reasonable request.

Conflicts of Interest: The authors declare no conflict of interest.

References

1. Zhao, Y.; Wang, X. A review of low-frequency active vibration control of seat suspension systems. *Appl. Sci.* **2019**, *9*, 3326. [CrossRef]
2. Kamesh, D.; Pandiyan, R.; Ghosal, A. Passive vibration isolation of reaction wheel disturbances using a low frequency flexible space platform. *J. Sound Vib.* **2012**, *331*, 1310–1330. [CrossRef]
3. Li, X.; Yan, Y.; Xu, Y.; Chen, W.; Shi, T.; Xia, C. Low-speed rotating restart and speed recording for free-running sensorless IPMSM based on ultrahigh frequency sinusoidal wave injection. *IEEE Trans. Power Electron.* **2022**, *37*, 15245–15259. [CrossRef]
4. Griffin, M.J. Vibration and motion. In *Handbook of Human Factors and Ergonomics*; John Wiley & Sons, Inc.: Hoboken, NJ, USA, 2012; pp. 616–637.
5. Davoodi, E.; Safarpour, P.; Pourgholi, M.; Khazaee, M. Design and evaluation of vibration reducing seat suspension based on negative stiffness structure. *Proc. Inst. Mech. Eng. Part C J. Mech. Eng. Sci.* **2020**, *234*, 4171–4189. [CrossRef]
6. Carletti, E.; Pedrielli, F. Tri-axial evaluation of the vibration transmitted to the operators of crawler compact loaders. *Int. J. Ind. Ergon.* **2018**, *68*, 46–56. [CrossRef]
7. Waters, T.; Rauche, C.; Genaidy, A.; Rashed, T. A new framework for evaluating potential risk of back disorders due to whole body vibration and repeated mechanical shock. *Ergonomics* **2007**, *50*, 379–395. [CrossRef]
8. Davoodi, E.; Safarpour, P.; Pourgholi, M.; Khazaee, M. A nonlinear seat suspension with high-static low-dynamic stiffness based on negative stiffness structure for helicopter. *J. Vib. Control* **2022**, *28*, 2879–2899. [CrossRef]
9. van Eijk, J.; Dijksman, J.F. Plate spring mechanism with constant negative stiffness. *Mech. Mach. Theory* **1979**, *14*, 1–9. [CrossRef]
10. Kochmann, D.M.; Bertoldi, K. Exploiting microstructural instabilities in solids and structures: From metamaterials to structural transitions. *Appl. Mech. Rev.* **2017**, *69*, 050801. [CrossRef]
11. Yang, J.; Xiong, Y.; Xing, J. Dynamics and power flow behaviour of a nonlinear vibration isolation system with a negative stiffness mechanism. *J. Sound Vib.* **2013**, *332*, 167–183. [CrossRef]
12. Zhang, Y.; Wei, G.; Wen, H.; Jin, D.; Hu, H. Design and analysis of a vibration isolation system with cam–roller–spring–rod mechanism. *J. Vib. Control* **2022**, *28*, 1781–1791. [CrossRef]
13. Fulcher, B.A.; Shahan, D.W.; Haberman, M.R.; Conner Seepersad, C.; Wilson, P.S. Analytical and experimental investigation of buckled beams as negative stiffness elements for passive vibration and shock isolation systems. *J. Vib. Acoust.* **2014**, *136*, 031009. [CrossRef]

14. Liao, X.; Zhang, N.; Du, X.; Zhang, W. Theoretical modeling and vibration isolation performance analysis of a seat suspension system based on a negative stiffness structure. *Appl. Sci.* **2021**, *11*, 6928. [CrossRef]
15. Li, H.; Li, Y.; Li, J. Negative stiffness devices for vibration isolation applications: A review. *Adv. Struct. Eng.* **2020**, *23*, 1739–1755. [CrossRef]
16. Xu, J.; Sun, X. A multi-directional vibration isolator based on Quasi-Zero-Stiffness structure and time-delayed active control. *Int. J. Mech. Sci.* **2015**, *100*, 126–135. [CrossRef]
17. Lu, Z.; Brennan, M.J.; Chen, L.Q. On the transmissibilities of nonlinear vibration isolation system. *J. Sound Vib.* **2016**, *375*, 28–37. [CrossRef]
18. Sarlis, A.; Pasala, D.; Constantinou, M.C.; Reinhorn, A.M.; Nagarajaiah, S.; Taylor, D.P. Negative stiffness device for seismic protection of structures: Shake table testing of a seismically isolated structure. *J. Struct. Eng.* **2016**, *142*, 04016005. [CrossRef]
19. Palomares, E.; Nieto, A.; Morales, A.; Chicharro, J.; Pintado, P. Numerical and experimental analysis of a vibration isolator equipped with a negative stiffness system. *J. Sound Vib.* **2018**, *414*, 31–42. [CrossRef]
20. Zha, J.; Nguyen, V.; Ni, D.; Su, B. Optimizing the geometrical dimensions of the seat suspension equipped with a negative stiffness structure based on a genetic algorithm. *SAE Int. J. Veh. Dyn. Stability NVH* **2022**, *6*, 147–158. [CrossRef]
21. Dong, G.; Zhang, X.; Xie, S.; Yan, B.; Luo, Y. Simulated and experimental studies on a high-static-low-dynamic stiffness isolator using magnetic negative stiffness spring. *Mech. Syst. Signal Process.* **2017**, *86*, 188–203. [CrossRef]
22. Wang, Q.; Zhou, J.; Wang, K.; Gao, J.; Lin, Q.; Chang, Y.; Xu, D.; Wen, G. Dual-function quasi-zero-stiffness dynamic vibration absorber: Low-frequency vibration mitigation and energy harvesting. *Appl. Math. Model.* **2023**, *116*, 636–654. [CrossRef]
23. Liu, C.; Zhang, W.; Yu, K.; Liu, T.; Zheng, Y. Quasi-zero-stiffness vibration isolation: Designs, improvements and applications. *Eng. Struct.* **2024**, *301*, 117282. [CrossRef]
24. Ye, K.; Ji, J. An origami inspired quasi-zero stiffness vibration isolator using a novel truss-spring based stack Miura-ori structure. *Mech. Syst. Signal Process.* **2022**, *165*, 108383. [CrossRef]
25. Liu, C.; Yu, K. Accurate modeling and analysis of a typical nonlinear vibration isolator with quasi-zero stiffness. *Nonlinear Dyn.* **2020**, *100*, 2141–2165. [CrossRef]
26. Tang, L.; Ren, N.L.; Funkhouser, S. Semi-active Suspension Control with PSO Tuned LQR Controller Based on MR Damper. *Int. J. Automot. Mech. Eng.* **2023**, *20*, 10512–10522. [CrossRef]
27. Hoang, V.N.; Deng, F.; Van, C.N. Adaptive optimal control system design for semi-active suspension system by supposing variable parameters under exogenous road disturbance. *Control Theory Technol.* **2024**, 1–10. [CrossRef]
28. Zhao, F.; Ji, J.; Ye, K.; Luo, Q. An innovative quasi-zero stiffness isolator with three pairs of oblique springs. *Int. J. Mech. Sci.* **2021**, *192*, 106093. [CrossRef]
29. Sun, X.; Zhang, J. Displacement transmissibility characteristics of harmonically base excited damper isolators with mixed viscous damping. *Shock Vib.* **2013**, *20*, 921–931. [CrossRef]
30. Xing, Z.Y.; Yang, X.D. A combined vibration isolation system with quasi-zero stiffness and dynamic vibration absorber. *Int. J. Mech. Sci.* **2023**, *256*, 108508. [CrossRef]
31. Karnopp, D.; Crosby, M.J.; Harwood, R. Vibration control using semi-active force generators. *J. Eng. Ind.* **1974**, *96*, 619–626. [CrossRef]